Available online at www.sciencedirect.com
SCIENCE DIRECT®
ELSEVIER
Journal of Chromatography A, 987 (2003) 39–48
JOURNAL OF CHROMATOGRAPHY A
www.elsevier.com/locate/chroma

Experimental Van Deemter plots of shear-driven liquid chromatographic separations in disposable microchannels

Nico Vervoort*, David Clicq, Gino V. Baron, Gert Desmet
Vrije Universiteit Brussel, Department of Chemical Engineering, Pleinlaan 2, 1050 Brussels, Belgium

Abstract

We present a new stationary phase coating method, yielding a monolayer of densely arrayed porous HPLC beads (d_p=4 μm) for use in a disposable shear-driven flow LC system. The system is inherently suited for whole-column detection through the small voids between the individual particles of the layer. The chromatographic performance of the system has been characterized by performing a series of coumarin dye separation experiments (reversed-phase mode) and by measuring the theoretical plate height as a function of the mobile phase velocity. The resulting Van Deemter curve, yielding a value of about 90 000 plates/m near the $u=u_{opt}$ velocity, shows good agreement with the theoretical expectations, and hence constitutes the first full validation of the theory of shear-driven chromatography.

Keywords: Shear-driven chromatography; Plate heights; Instrumentation; Flow velocities; Polyethoxysilane

1. Introduction

Due to the increased demand for chemical and biological analyses coming from the chemical and pharmaceutical research sector [1,2], the past decade has witnessed tremendous research efforts aiming at the development of novel analytical methods yielding shorter analysis times and increased sample throughputs [3]. One of the most promising concepts that evolved from the work in this field was that of the so-called micro-total analysis systems (μ-TAS) also referred to as laboratory-on-a-chip [4–6]. A typical μ-TAS system integrates a variety of functionalities, such as micromixers, microreactors, separation channels, immunoassay sensors, etc. on the surface of a single silicon or glass wafer, and is capable of analysing small sample volumes in a time scale 10–100× faster than most conventional techniques. These miniaturized systems generally offer a greatly improved analysis speed and sample throughput, reduced costs and reagents consumption and the possibility of parallel and integrated analysis. Furthermore, the possibility of mass production at low cost opens a tremendous potential for applications in genomics, proteomics, drug discovery and medical diagnosis [7].

One of the main challenges in the development of these microfluidic devices however remains the generation of the flow through the microchannels. Due to their small dimensions, microchannels generally generate a large pressure drop. The relatively poor mechanical strength of the devices and the still unresolved pump connection problems furthermore often limit the applicable inlet pressure to a few tens of bars, such that only low pressure driven flow-rates can be established. The flow in most μTAS applica-

*Corresponding author. Tel.: +32-2-629-3617; fax: +32-2-629-3248.
E-mail address: nvervoor@vub.ac.be (N. Vervoort).

0021-9673/02/$ – see front matter
PII: S0021-9673(02)01905-2

tions is therefore driven by the application of a voltage gradient to create an electroosmotic flow (EOF). Electrically-driven flows however also display a number of disadvantages [8]: the flow velocity fluctuates with slight changes of the ionic strength and the viscosity of the fluid, the effect of Joule heating imposes and upper limit on the applicable voltage gradient, the double-layer overlap and the accompanying decrease of the achievable fluid velocity [9] make it difficult to exploit the kinetic advantages of sub-μm thin channels, etc.

In an attempt to overcome these problems, our group has proposed an alternative way of transporting fluids through microchannels, i.e. by making use of shear-driven flows [10]. The shear-driven flow principle is based on the use of channels which are divided into two, non-sealed and independently moving parts. By axially sliding one part of the channel past the other, the viscous drag effect establishes a net flow with a linear velocity gradient. One of the interesting properties of shear-driven flows is that the average fluid velocity is independent of the length and the thickness of the channels and of the physical properties of the fluid, but is always exactly equal to one half of the velocity of the moving wall. Shear-driven flows are hence also intrinsically more robust than electrically-driven flows, where the fluid velocity tends to fluctuate with small changes of the physico–chemical properties of the mobile or stationary phase [11]. One of the possible applications of shear-driven flows we looked at thus far is liquid phase chromatography (LC), but the flow principle certainly can also be used in a multitude of other applications, including, e.g. DNA micro-array screening, flow-through immunoassays, etc. The reason for our current focus on LC is the large potential gain margin with respect to the currently used pressure-driven method (HPLC). It is namely a well-established fact [12,13] that, if there would be no limitation on the mobile phase velocity, it should be possible to decrease the analysis time t_R in LC according to the second power of the channel depth or particle diameter ($t_R \sim d^2$). Since shear-driven flows are much better suited to reconcile a large fluid velocity and a small (preferably sub-μm) channel thickness than electrically- or pressure-driven flows, it should hence be obvious that they potentially offer a large gain in separation speed, as has been quantitatively demonstrated in [14].

To explore the practical feasibility of shear-driven flow LC (SDC), we first performed a series of tracer flow experiments [10], allowing us to demonstrate that it is indeed possible to generate unidirectional flows with velocities up to 2 cm/s through channels as thin as 100 nm, without the aid of an external pressure or voltage gradient. Subsequently, we performed a series of low-resolution separations of Rhodamine B/PN Black 151 in laser-jet printed disposable microchannels [15]. The employed stationary-phase consisted of HPLC silica beads which were embedded in a polyacrylic polymer layer to immobilize them on the surface of the stationary wall of the shear-driven flow channels. The thickness of the layers was not very reproducible and varied between 6.5 and 20 μm. Another drawback of the adopted approach was that, together with some overloading problems, the presence of the polymer matrix gave rise to theoretical plate height values which were in some cases up to two to three times larger than the theoretically expected value, given by Ref. [14]:

$$H = 2\frac{D_m}{u} + \frac{2}{30}\frac{1 + 7k + 16k^2}{(1+k)^2}u\frac{d^2}{D_m} + \frac{2}{3}\frac{k}{(1+k)^2}u\frac{d_f^2}{D_s} \quad (1)$$

In the present paper, we report on a new coating method, yielding a stationary phase consisting of a monolayer of homogeneously distributed HPLC beads, attached to the surface of a glass slide using a nanometrically thin layer of polyethoxysilane (PES), hence avoiding the need for the polymeric embedding matrix. Since the produced stationary phase is chemically and physically identical to the stationary phases used in HPLC, this approach offers the advantage that existing HPLC separation protocols can be directly adopted and that a direct comparison between shear-driven and pressure-driven LC becomes possible. Furthermore, the obtained layers are thinner than with the previous method, and the absence of a polymer matrix yields an additional reduction of the stationary phase mass transfer resistance. It can hence be expected that the pro-

duced layers will yield smaller theoretical plate height values than the layers produced with our previous method.

2. Experimental

2.1. Chemicals

Tetraorthosilicate (TEOS, CAS No. 78-10-4) 99% pure, dimethyloctadecylchlorosilane (CAS No. 14799-93-0) and sodium tetraborate (CAS No. 1330-43-4) were obtained from Fluka (Belgium). Ethanol (LiChrosolv), hydrochloric acid, potassium hydroxide and superspher Si 60 (4 μm, normal-phase) were obtained from Merck (Darmstadt, Germany). Toluene, methanol and acetonitrile (all HPLC-grade) were obtained from Aldrich (Steinheim, Germany). Coumarin 440 (CAS No. 26093-31-2) and coumarin 460 (CAS No. 91-44-1) were obtained from Acros Organics (Geel, Belgium).

2.2. Chromatographic set-up and procedure

The set-up used in the present study is depicted in Fig. 1. The heart of the set-up is a disposable shear-driven channel unit, consisting on the one hand of a commercial transparency sheet (Ahrend No 38 87 91, Germany), serving as the moving channel wall and carrying two parallel, 8 μm thick carbon strips, obtained by printing them onto the surface of the transparency sheet with a commercial laser-jet printer (HP LaserJet 1100). These lines extended over the entire length of the transparency sheet and formed the side-walls of the channels. Closing the thus obtained half-open channels by putting a conventional microscope slide on top of the printed toner lines, a ready-to-use and very cheap SDC-channel system is obtained. During the operation, the transparency sheet was fixed onto a commercial glass plate serving as the support. The channels were filled by capillary action, by simply putting a drop of mobile phase just in front of the channel inlet. This method prevents the insertion of air bubbles into the column. A stock solution of 5 m*M* of coumarin 440

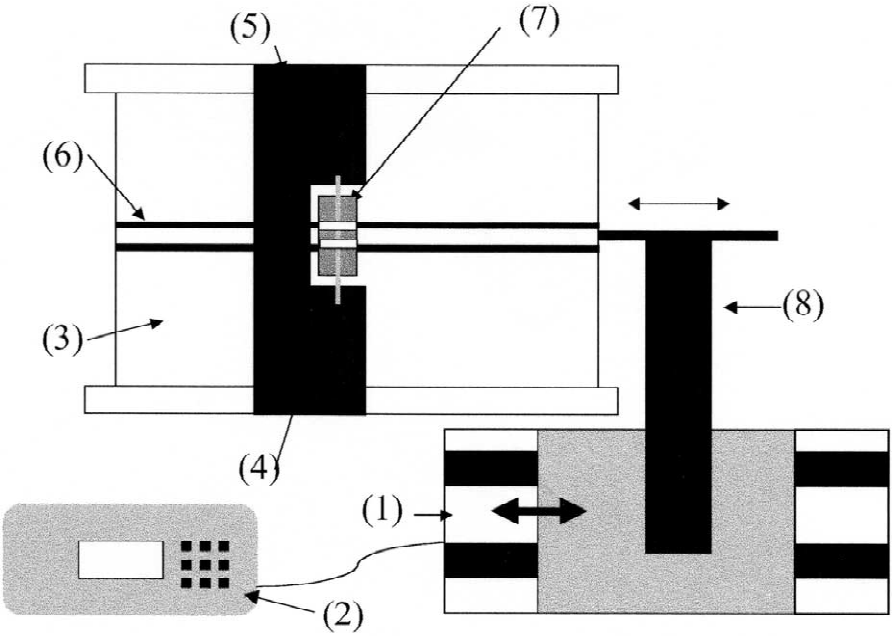

Fig. 1. Top view of the SDC setup: (1) axial displacement system; (2) digital controller; (3) moving channel wall; (4) stationary slide holder; (5) guidance rail; (6) printed channel on transparency sheet; (7) SDC column; and (8) connection piece. The UV excitation lamp and the CCD camera (both not represented here) are respectively positioned directly above and underneath the SDC column.

and coumarin 460 in methanol was made (due care should be taken when manipulating these compounds since their chemical and physical properties have not fully been investigated and they are suspected carcinogens) and then further diluted with mobile phase to a mixture containing 1 m*M* of both compounds. A small amount was injected by putting a drop of this mixture in front of the channel inlet and displacing the moving channel wall about 1 mm, yielding an injection plug length of about 500 μm. The non-entered sample was flushed away with buffer solution. Because of the huge flow resistance inside the channel, this flushing action can be performed without disturbing the injected sample plug. After injection of the sample plug, the motion of the channel is started and the chromatographic run begins. The axial displacement of the moving wall was controlled by an automated displacement system (M-TS100 DC.5, Newport, The Netherlands), offering a stepping accuracy of 0.5 μm and a speed range between 1 μm/s and 10 cm/s. Excitation of the fluorescent dyes was accomplished by a common UV ''black light'' with a 360 nm bandpass filter (Exciter D360/50, AHF Analysentechnik, Tübingen, Germany) in front of the lamp. This lamp was placed directly above the channel. The chromatographic runs were visualized with a black and white charge-coupled device (CCD) camera (ORCA ER C4742-95, Hamamatsu Photonics, Belgium), connected to a computer equipped with a digital video capture card (Matrox Meteor II-dig, Matrox, USA) and accompanying software (Simple-PCI 4.0). To reduce the background from the UV lamp, a filter with a cut-on of 400 nm (FSQ-GG400, Newport) was placed in front of the camera. This also offered the advantage that the complete channel was always visualized and that a run could be stopped after baseline separation of the analytes. At regular intervals, still images were captured from the video sequence. These images were fed to a self-written MATLAB routine, capable of reading the intensity of each pixel of the image. The intensity was averaged over the width of the channel and plotted vs. the axial direction, yielding a chromatogram of the analyte intensity in the spatial domain instead of in the time domain, which is more customary in LC. All experiments where conducted at ambient temperature (T~20 °C), using an acetonitrile–10 m*M* natrium tetraborate (50:50, v/v) mixture as the mobile phase. After every run the column was thoroughly rinsed with methanol and dried with pressurized air to prevent carry-over of analyte between different runs.

2.3. Coating of substrates with RP stationary phase

Hydrolyzed PES was prepared by mixing a catalytic solution containing 6.5 ml deionized water and 70 μl hydrochloric acid with 50 ml TEOS dissolved in 30 ml ethanol. The reaction was allowed to proceed for 16 h at room temperature. The residual water, catalyst and ethanol were removed under vacuum until the volume was about 50% of the original volume. The PES solution was then centrifuged at 2500 rev./min for 15 min to remove any solid particles and the supernatant was used as PES stock solution. Before using them as a substrate, the microscope slides were cleaned with detergent and put in 1 *M* KOH for 3 h to create a maximum of free hydroxyl groups on the surface. After sufficient rinsing with deionized water, the slides were dried for 1 h at 120 °C. Prior to applying the HPLC beads, the surface of the microscope slides was coated with a thin layer of hydrolyzed polyethoxysilane by dip-coating a clean microscope slide with a 10% PES stock solution in ethanol. After evaporation of the solvent, the remaining PES layer remains slightly ''gelly'', and can hence be used as a ''glue'' for the HPLC beads. The latter were applied onto the surface of the microscope slide using a simple spatula and by removing the non-bonded particles with pressurized air. This procedure led to the deposition of a monolayer of HPLC beads onto the substrate (Fig. 2a and b). After aging of the coatings in an ammonia atmosphere for 3 h, and after having rinsed them with water, the beads were found to be firmly attached to the glass slide and were then silanized by reacting them for 12 h in a 5% solution of dimethyloctadecylchlorosilane (C_{18}) in toluene. After the silanization reaction, the slides where rinsed with toluene and methanol to remove residual reagents and dried in an oven at 120 °C for 2 h. The thus obtained finished stationary phase layers had a well-defined thickness (monolayer of beads) and porosity and were hence much more reproducible

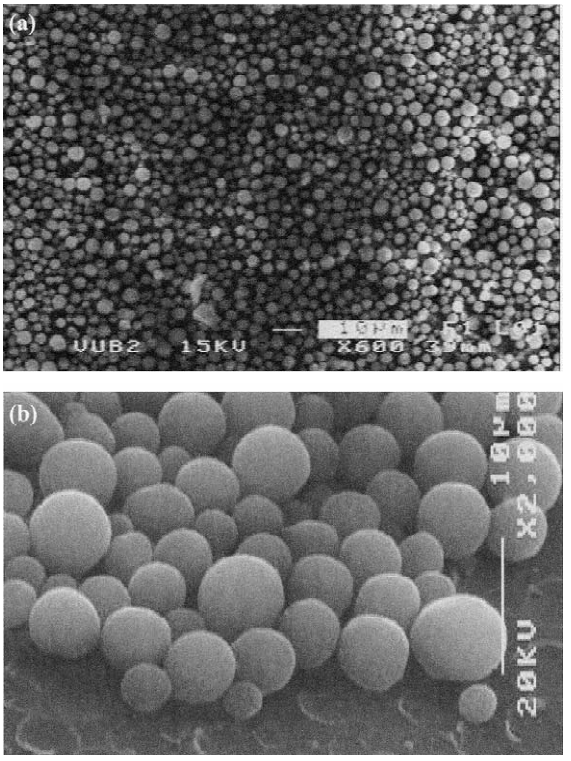

Fig. 2. Top view (a) and close-up (b) of monolayer of HPLC beads coated on microscope slide.

than the polymer/silica stationary phase layers we used previously [15].

3. Results

Fig. 2 shows two scanning electron microscopy (SEM) photographs of one of the prepared stationary phase layers. It can clearly be noted that the particles are packed closely together, resulting in an almost 100% coverage of the slide surface with particles. It should be noted here that the figure of 100% refers to the value of the maximally attainable relative surface coverage, which can, by considering a densely packed array of identical cylinders with uniform diameter, be calculated to be equal to $\pi/(2\sqrt{3}) \cong 0.91$. Theoretically, the height of the layer should be very uniform, as the bonding chemistry has been selected such that the silica beads only form a monolayer, i.e. the particles only bind to the surface of the microscope slide and not to each other. Fig. 2a,b clearly confirm this, but they however also show a quite large variation on the size of the individual beads, and hence also of the local layer thickness. As the local layer thickness variance is fully caused by the poor particle size uniformity of the employed commercial bead sample, this is a problem which should be easy resolvable, i.e. by switching to a more uniform bead sample. From Fig. 2b, it can be estimated that the PES layer is maximally a few 100 nm thick, hence ascertaining that the PES layer only minimally disturbs the functioning of the HPLC beads. Cracking of the deposited PES layer could be observed when the PES concentration in the coating solution exceeded 30%. At this concentration the layer thickness becomes too large to withstand the capillary forces acting on the layer when the solvent is evaporating.

The mechanical properties of the prepared coatings were very good. The particles were firmly attached to the slide, and were even found to withstand manual scrubbing of the surface. Very little wear could be observed when using the slides with pure aqueous solutions. When using the layers in combination with the mobile phase used during our separation experiments, we however experienced a relatively large percentage of faulty runs (about 20%), marked by the generation of an abnormal flow pattern of the analytes. Most of the failures were caused by clusters of toner particles coming from the channel side-walls and entering the channel, hence lifting the microscope slide and scratching the stationary phase layer. The detachment of the toner particles was caused by the relative high concentration of acetonitrile in the mobile phase, causing the carbon toner particles to gradually dissolve. As a consequence, the laser-jet printed moving channel parts only had a limited lifetime, and had to be replaced after about 10 runs. The stationary phase on the microscope slides on the other hand performed very well, since all experiments (about 60 runs) could be conducted with only three stationary phase slides and no degradation of separation efficiency could be observed during the operation of each of the slides. The only reason why the stationary phase slides needed to be replaced was the formation of scratches caused by the shear of detached carbon particle clusters, as already mentioned.

For each of the completed runs, the retention factor k was calculated from a video frame taken immediately after the injection of the sample plug (Fig. 3a) and one taken at the moment where the leading peak had elapsed a distance of about 1.5 cm (Fig. 3b). Fig. 3b clearly evidences that a full baseline separation of the two coumarin dyes could easily be obtained. In general, it was observed that, when operating the system at the maximal mobile phase velocity of 1 mm/s, the baseline separation of the two dyes could be accomplished within about 30 s.

Denoting the distance elapsed by the unretained mobile phase fluid by L_0, and denoting the distance travelled by the sample components by L_{eff} (Fig. 3c), the value of the retention factor k can be directly calculated using [15]:

$$k = \frac{L_0 - L_{\text{eff}}}{L_{\text{eff}}} \tag{2}$$

Since the peak of coumarin 440 had a retention factor of $k \cong 0$, the distance travelled by this peak was taken as L_0. The average retention coefficient for the coumarin 460 peak was found to be given by:

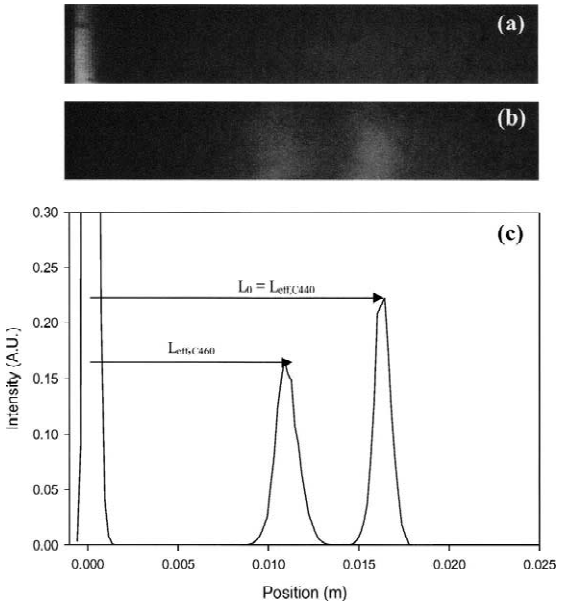

Fig. 3. Still image of injection peak (a), still image of baseline separated coumarin 440 and coumarin 460 peaks (b), overlaid pixel intensity plots of both still images (c).

$$k = 0.42(\pm 0.097) \tag{3}$$

No statistically significant difference between the three employed stationary phase coatings could be observed, i.e. the run-to-run variability of the retention factor was already so large that it masked any coating-to-coating variability.

Experimental plate height values were estimated from the colour intensity plots (Fig. 3c) derived from the still images, using the difference between the variance σ_x^2 of the sample component peaks and the variance of the injected peak $\sigma_{x,\text{inj}}^2$:

$$H = \frac{\sigma_x^2 - \sigma_{x,\text{inj}}^2}{L_{\text{eff}}} \tag{4}$$

Varying the velocity over a relatively broad range (0.08 mm/s$<u<$1 mm/s), and repeating the experiment eight times for each investigated values of the velocity, a full Van Deemter plot could be established (Fig. 4). As can be noted, the experimental H-values agree well with the theoretical prediction obtained by respectively putting $k=0$ and $k=0.4$ in Eq. (1).

4. Discussion

The ease of column regeneration and column replacement was found to be one of the most prominent advantages of the presently proposed system. After each run, the microscope slide carrying the stationary phase layer can simply be lifted from the moving wall part, and can be subjected to any desired regeneration process, or can simply be disposed off to exclude any carry-over effect.

Previous measurements of the separation efficiency of SDC using the polymer/silica stationary phase described in [15] gave a plate height of about two to three times the theoretical expected plate height. This was in part explained by the fact that we needed to overload the column to obtain a sufficient detection sensitivity with our then used visible range CCD camera detection system. By switching to fluorescence detection, the detection sensitivity obviously increased, allowing to reduce the concentration of the injected analytes (20 mM for the Rhodamine B/PN Black 151 separations presented in Ref. [15]

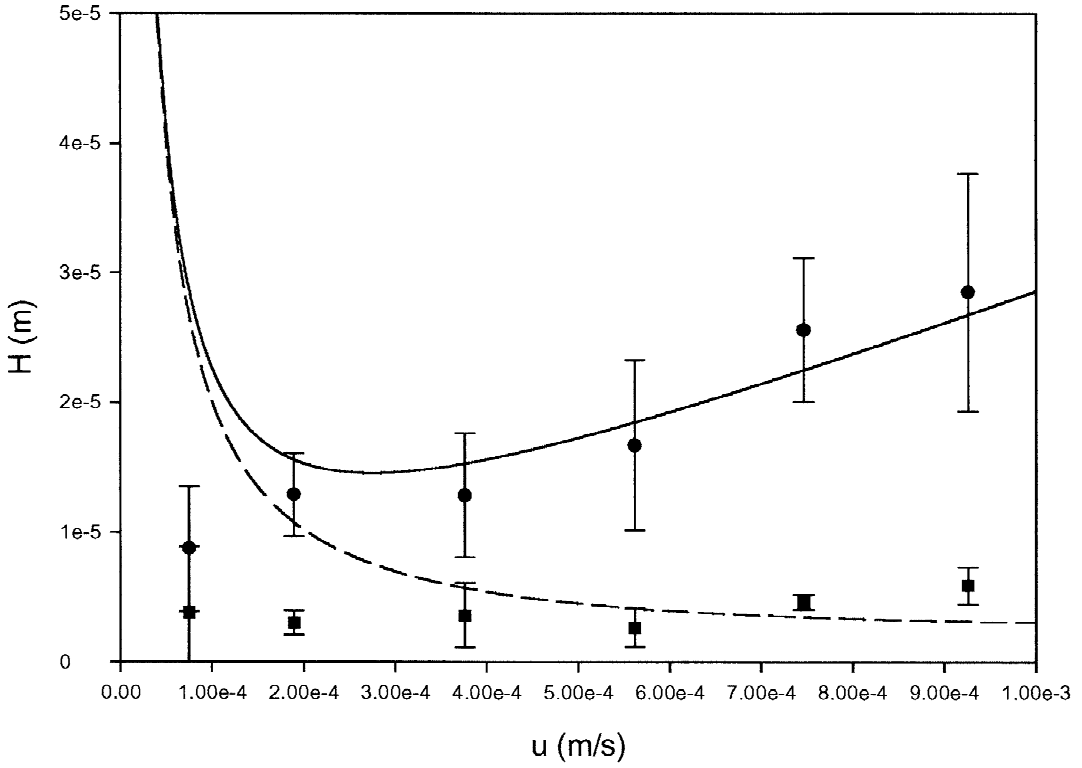

Fig. 4. Van Deemter plot showing experimental H values for coumarin 460 (●) and coumarin 440 (■) and the theoretical expected values for a compound with $k=0.4$ (———) and $k=0$ (- - -), obtained by respectively putting $k=0.4$ and $k=0$ in Eq. (1). Values of the other parameters: $d_f=4\cdot10^{-6}$ m, $d=8\cdot10^{-6}$ m, $D_m=10^{-9}$ m^2/s, $D_s=10^{-10}$ m^2/s.

vs. 1 mM in the present study). From the fact that the presently established Van Deemter plot (Fig. 4) is in good agreement with the theoretical expression given in Eq. (1), we can safely state that the overloading problem we previously experienced now has been eliminated. It should be noted that the theoretical curves have been established by using the nominal particle diameter value of the employed HPLC beads ($d_p=4$ μm) as the value for the stationary phase thickness d_f in Eq. (1). This probably is not entirely correct, since, as can be noted from Fig. 2, a large fraction of the particles is considerably smaller than this nominal value. This probably explains why the majority of the experimental H values in fact lies slightly below the theoretical curve. The variance of the measured H values is well within acceptable limits, and is most probably caused by the relatively crude detection method. It was namely found to be extremely difficult to exactly restore the channel illumination conditions from run-to-run, and this lead to a considerable variance on the observed concentration profiles (with more background radiation, the peaks tend to appear smaller than they actually are). We suspect that the large variance on the retention factor values (cf. Eq. (3)) is due to the fact that during some runs the microscope slide was lifted by the detaching carbon toner particles coming from the side walls.

Around the optimum velocity, a plate count of about 90 000 plates/m is obtained (Fig. 4). As is evidenced in Fig. 5, the theoretical plate height values obtained with the present shear-driven chromatography system (total channel depth = 8 μm and stationary phase thickness = 4 μm) are comparable to those achievable with conventional HPLC using 4 μm particles. The HPLC data given in Fig. 5 have been obtained from the well-known Katz equation [16]:

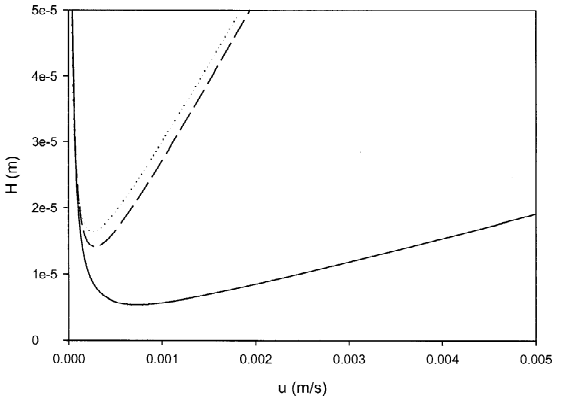

Fig. 5. Van Deemter plot showing a theoretical comparison between HPLC and SDC systems; (·····) HPLC employing 4 μm beads; (- - -) SDC system employing a stationary phase of 4 μm and a total channel depth of 8 μm; (———) SDC system employing a stationary phase of 1.5 μm and a total channel depth of 3 μm. The SDC data were obtained from Eq. (1), the HPLC data were obtained from Eq. (5), using $d_p = 4 \cdot 10^{-6}$ m, $D_m = 10^{-9}$ m^2/s, $D_s = 10^{-10}$ m^2/s, $k = 0.4$, $\lambda = 0.5$ and $\gamma = 0.8$.

$$H = 2\lambda d_p + 2\gamma \frac{D_m}{u} + \frac{0.37 + 4.96k + 4.04k^2}{(1+k)} u \frac{d_p^2}{D_m} \quad (5)$$

known to yield H values which are very similar to those predicted by the Knox equation [17].

Whereas in HPLC, the further decrease of the particle size is limited because of the pressure-drop restrictions [18] this is no issue at all for a shear-driven system. For example, by switching to a monolayer of 1.5 μm particles, and by reducing the total channel thickness to about 3 μm, it should be possible to decrease the currently obtained plate height values by a factor of 3, as can be derived from a comparison between the full and the dashed SDC curves in Fig. 5. From the much flatter slope of the Van Deemter curve in the large u range, it can also be inferred that switching to thinner layers will also allow to considerably speed up the analysis. Future experiments are planned to verify this prediction, together with the consideration of more difficult separation problems, such as the separation of complex mixtures of polyaromatic hydrocarbons or fluorescently labeled proteins. Reduction of the channel thickness will not pose a problem since microchannels can be etched at almost any desired depth into glass substrates using etching techniques adopted from microelectronics fabrication [19]. Apart from the use of μm- or sub-μm sized beads for the creation of thinner stationary phase layers, we will also explore the possibilities of the currently available sol–gel [20] and surface anodization techniques [21] for the creation of thin, homogeneous (i.e. not consisting of individual beads) stationary phase layers.

The poor chemical resistance of the currently used laser-jet printed channels clearly is a problem. However, with the presently available μprinting and plastic replication techniques [22–24] it should be possible to manufacture channel systems which are much less prone to dissolution in organic solvents. One possible solution would be to replace the carbon particles from the printer toner by particles of a more resistant material (e.g. metallic or inorganic). Another solution would be to hot emboss the desired channel shape into a polymeric sheet. Both solutions have a clear advantage over the other obvious solution to produce chemically resistant microchannels, i.e. wet-etching of the channel in a large glass-plate, because they are extremely cheap and are intrinsically suited for mass scale production.

Although the detection sensitivity of the current set-up was sufficient to eliminate the column overloading problems we experienced previously [15], the fact that the UV lamp used for illumination of the channel was directly above the CCD camera lead to a relatively high background signal, such that the full potential of the CCD camera could not be used. In our future experiments, we will therefore switch to an alternative layout, already described in [25] and based on the use of a fluorescence microscope.

Due to its flat format, the system is inherently suited for whole-column detection, allowing to operate it with the same degree of visual control as in thin layer chromatography (TLC). Because of the small voids between the particles, the particle layer is highly transparent for both the excitation light and the emitted fluorescence light. If required, a UV-absorption detection cell can be integrated at the end of the column, as described in [25]. For this application, the flat-rectangular format of the channel, offering an optical path length of the order of a few millimeter, is highly advantageous.

5. Conclusion

We have presented a novel coating method to apply silica particles on a flat rigid substrate for use as a stationary phase in shear-driven chromatography. The bonding chemistry, based on the formation of siloxane bonds between the PES coating and the free hydroxyl groups on the silica beads, has been selected such that the silica particles only bond to the surface of the glass slide, and not to each other, hence guaranteeing to yield a perfect monolayer. The method also offers the advantage that the chemical and the physical properties of the stationary phase are identical to those used in HPLC, allowing a direct transposition of the separation protocols. Using the prepared stationary phase layers in combination with a previously developed laser-jet printed channel system, a low-cost disposable LC system is obtained. Due to its flat format and the open-channel architecture, the system in fact offers a mixed form of the functionalities of both TLC and HPLC. The operation mode (complete elution of the components) and the high separation resolutions are similar to that of HPLC, whereas the possibility for whole-column detection and the ease of column regeneration and replacement is similar to TLC. The system is hence also ideally suited to support the development of novel HPLC routines.

The separation performance of the established system could be quantified by means of a Van Deemter plot, showing good agreement with the theoretical expectations, and hence constituting the first full validation of the theory of shear-driven chromatography. Using 4 μm beads in an 8 μm deep channel we are able to obtain about 90 000 plates/m for a compound with a retention factor k of about 0.4. This result is comparable to the number of theoretical plates which can be obtained with an HPLC column packed with 4 μm particles.

The performance of the system obviously can be further improved by: (i) switching to more appropriate printing techniques for the formation of the channel side-walls to omit the problem of the poor chemical resistance of the currently used carbon toner particles; (ii) reducing the thickness of the stationary phase layers, e.g. by applying smaller HPLC beads; and (iii) improving the uniformity of the layers, by applying more uniform bead samples, or by resorting to existing sol–gel or surface anodization techniques.

6. Nomenclature

d	total channel thickness (m)
d_f	stationary phase thickness (m)
d_p	particle diameter (m)
D_m	molecular diffusion coefficient (m^2/s)
D_s	molecular diffusion coefficient in the stationary phase (m^2/s)
H	height of equivalent theoretical plate (m)
k	retention factor (–)
N	theoretical plate number (–)
u	mean mobile phase velocity (m/s)
u_{wall}	velocity of moving wall (m/s)
x	axial coordinate (m)

Greek

σ_x^2	peak variance in the space domain (m^2)
λ	geometric factor in A term of Van Deemter equation
γ	tortuosity in B term of Van Deemter equation

Subscripts

col	column
eff	effective
exp	experimental
inj	injection
theo	theoretical
opt	optimal

References

[1] J.M. Bruin, Electrophoresis 21 (2000) 3931.
[2] E. Verpoorte, Electrophoresis 23 (2002) 677.
[3] D. Figeys, D. Pinto, Anal. Chem. 72 (2000) 330A.
[4] D.J. Harrison, K. Fluri, K. Seiler, Z.H. Fan, C.S. Effenhauser, A. Manz, Science 261 (1993) 895.
[5] A. Manz, D.J. Harrison, E. Verpoorte, J.C. Fettinger, A. Paulus, H. Lüdi, H.M. Widmer, Adv. Chromatogr. (1993).

[6] D.R. Reyes, D. Iossifidis, P.-A. Auroux, A. Manz, Anal. Chem. 74 (2002) 2623.
[7] J. Khandurina, A. Guttman, J. Chromatogr. A 943 (2002) 159.
[8] W. Kok, Chromatographia 51 (Suppl) (2000) S28.
[9] L.B. Bhuiyan, C.W. Outhwaite, S. Levine, Chem. Phys. Lett. 66 (1979) 321.
[10] G. Desmet, G.V. Baron, Anal. Chem. 72 (2000) 2160.
[11] A.L. Crego, J. Martinez, M.L. Marina, J. Chromatogr. A 869 (2000) 329.
[12] G. Guiochon, J. Chromatogr. 185 (1979) 3.
[13] J.H. Knox, M.T. Gilbert, J. Chromatogr. 186 (1979) 405.
[14] G. Desmet, G.V. Baron, J. Chromatogr. A 855 (1999) 57.
[15] G. Desmet, N. Vervoort, D. Clicq, G.V. Baron, J. Chromatogr. A 924 (2001) 111.
[16] E.D. Katz, K. Ogan, R.P.W. Scott, in: F. Bruner (Ed.), The Science of Chromatography—Lectures presented at the A.J.P. Martin Honorary Symposium, Urbino, 27–31 May 1985 (Journal of Chromatography Library, Vol. 32), Elsevier, Amsterdam, 1985, p. 403.
[17] P.A. Bristow, J.H. Knox, Chromatographia 10 (1977) 279.
[18] H. Poppe, J. Chromatogr. A 778 (1997) 3.
[19] A. Manz, J.C. Fettinger, E. Verpoorte, H. Lüdi, H.M. Widmer, D.J. Harrison, Trends Anal. Chem. 10 (1991) 144.
[20] S. Constantin, R. Freitag, J. Chromatogr. A 887 (2000) 253.
[21] J. Drott, K. Lindstrom, L. Rosengren, T. Laurell, J. Micromech. Microeng. 7 (1997) 14.
[22] Y. Xia, J.J. McCelland, R. Gupta, D. Qin, X. Zhao, L.L. Shon, R.J. Celotta, G.M. Whitesides, Adv. Mater. 9 (1997) 147.
[23] E. Kim, Y. Xia, G.M. Whitesides, Nature (Letters to) 376 (1995) 581.
[24] T. Boone, Z.H. Fan, H. Hooper, A. Ricco, H.D. Tan, S. Williams, Anal. Chem. 74 (2002) 78A.
[25] G. Desmet, N. Vervoort, D. Clicq, A. Huau, P. Gzil, G.V. Baron, J. Chromatogr. A 948 (2002) 19.